Relaxation of Randomly Cross-Linked Polymer Melts

Edgardo R. Duering

Max Planck Institut für Polymerforschung, 6500 Mainz, Germany

Kurt Kremer

Institut für Festkörperforschung, Forschungszentrum Jülich, Germany [a]
and Department of Chemical Engineering and Materials Science, University of Minnesota, Minneapolis, Minnesota 55455

Gary S. Grest

Corporate Research Science Laboratories, Exxon Research and Engineering Company, Annandale, New Jersey 08801
(Received 12 August 1991)

The dynamical properties of randomly cross-linked polymer melts, far above the vulcanization threshold, are studied using molecular-dynamics simulations. The mean-square displacements of the middle and end monomers of the chains as well as the cross-links are considered. The dynamic scattering function $S(q,t)$ as measured by neutron spin echoes is also calculated. The average strand length between two cross-links is about $\frac{1}{4}$ of the entanglement length of the un-cross-linked melt. By introducing a new intermonomer potential, we can explicitly test the influence of trapped entanglements. For the present system, the frozen entanglements change the plateau modulus by about 25%.

Recently there has been a significant experimental [1] and theoretical effort [2] to understand the relaxation behavior of cross-linked polymer systems. Cross-linked polymers, such as a gel or rubber, are the basis for most industrial macromolecular products as well as the stabilizing structure in many biological systems. Thus a detailed understanding of such systems is highly desirable and a subject of intense research for more than fifty years [3]. The difficulty with understanding rubber is that it depends on a variety of parameters, including the cross-linking procedure, the number of cross-links, and the number of trapped entanglements. The number of cross-links determines the average strand length and the distribution of strand lengths N_s between two cross-links. The strand-length distribution plays an important role in determining the elastic and relaxational properties of the system. Topologically trapped entanglements are also thought to play an important role, particularly when the average strand length is much longer than the entanglement length of the un-cross-linked melt. Since the constraints are permanent, the system is nonergodic and relaxation is very slow. Experimentally, a detailed understanding of how rubber relaxes has been slow in developing, since it is difficult to produce networks under conditions which allow a clear specification of the distribution of strand lengths N_s and the number of trapped entanglements. Analytic theories of rubber are complex and are often forced to make a number of very serious, untested approximations in order to proceed. The role of entanglements in particular is poorly understood [2].

In a simulation it is possible to modify the cross-linking procedure in order to produce a variety of networks. Possible systems range from randomly cross-linked melts to regular lattice structures, where the lattice bonds are replaced by polymer chains of constant length. One can also use different interaction potentials, which either allow the chains to cut through each other or not. By con-

struction these potentials can have the same second virial such that the contribution of the conserved chain topology can be directly evaluated. In this Letter we report the first results of an extended series of simulations on cross-linked polymer networks.

Here we only consider randomly cross-linked polymer melts far above the vulcanization threshold. Most of the chains (96%) are in the infinite network. This situation probably most closely resembles the case of radiation cross-linking. The initial configurations are equilibrated polymer melts (M chains of N monomers), similar to those used in earlier studies on the dynamics of entangled polymers [4]. The chains are in a cubic box with periodic boundary conditions. All monomers interact via a purely repulsive Lennard-Jones (LJ) potential,

$$U^{LJ}(r) = \begin{cases} 4\epsilon\{(\sigma/r)^{12} - (\sigma/r)^6 + \frac{1}{4}\}, & r \leq r_c, \\ 0, & r > r_c, \end{cases} \tag{1}$$

where $r_c = 2^{1/6}\sigma$. For subsequent monomers along the chain an anharmonic interaction [4,5] is added,

$$U^{ch}(r) = \begin{cases} -0.5R_0^2 k\{\ln[1-(r/R_0)^2]\}, & r < R_0, \\ \infty, & r \geq R_0, \end{cases} \tag{2}$$

where $k = 30\epsilon/\sigma^2$ and $R_0 = 1.5\sigma$. For temperature $k_B T/\epsilon = 1$ and density $\rho = N/V = 0.85\sigma^{-3}$ the entanglement length $N_e = 35$ [4]. The entanglement time τ_e (Rouse time of a subchain of length N_e) is roughly 1800τ, where $\tau = \sigma(m/\epsilon)^{1/2}$. In our molecular-dynamics simulation the monomers are weakly coupled to a heat bath and the corresponding friction coefficient $\Gamma = 0.5\tau^{-1}$. The integration of the equation of motion was carried out using a velocity Verlet algorithm [6,7] with time step $\Delta t = 0.0135\tau$. We studied six different polymer melts: five samples of 50 chains of $N = 50$ (50/50) and one large sample of 400 chains of $N = 50$ (400/50). The total length of the longest run was 40000τ. Here we study the case $p = 2$ cross-

links per chain (p_c =0.84 [8]). This gives an average of four cross-linked monomers per chain, dividing each chain into five segments on average [9]. The cross-linking was done by first randomly selecting a point in space. The nearest monomer to that point was then taken as one of the cross-linking sites. All monomers within a sphere of reaction radius r_x = 1.3σ [$\approx (c_\infty)^{1/2}$ of this system] were then enumerated. The first monomer was then bonded to one of the monomers within this reaction volume selected at random, provided it was not a nearest or second-nearest neighbor along the chain of the original monomer. This procedure was then repeated pM times. The networks had approximately the number of intra-chain connections predicted by Tonelli and Helfand [10]. The bond potential of a cross-link was taken to be the same as for the original chains, Eq. (2). For p =2 the average strand length N_s between two consecutive cross-links was $\langle N_s \rangle$ =8.9 $\pm$ 0.1 which is only $\frac{1}{4}$ of N_e for the corresponding melt. The average length of a dangling end $\langle N_d \rangle$ =11.6 $\pm$ 0.2 [9]. On average, 96% of the chains belong to the infinite network (the remaining monomers were free un-cross-linked chains) with about 46% of the monomers in dangling ends. We found that after removing the dangling ends most of the remaining monomers were elastically active.

One of the main problems in rubber elasticity is to separate the various contributions to the elastic modulus. While this is not possible experimentally, it can be done in a simulation by studying the same cross-linked melts with two interaction potentials. In this case the repulsive LJ potential for nonbonded monomers is replaced by a soft-core potential of the form

$$U^{\cos}(r) = \begin{cases} 2\epsilon_a, & r < r_a, \\ \epsilon_a \left[\cos \dfrac{\pi(r - r_a)}{r_c - r_a} + 1 \right], & r_a \le r \le r_c, \\ 0, & r > r_c. \end{cases} \quad (3)$$

r_a and ϵ_a are chosen so that the chains in the un-cross-linked melt have the same persistence length, pressure, and Rouse friction as for the LJ potential. For ρ =0.85σ^{-3}, r_a = 1.0σ and ϵ_a =2.22ϵ. R_0 in Eq. (2) was increased to 1.75σ and the overall interaction between connected monomers along the chain was reduced by a factor of 0.175 [7]. With this interaction, monomers can now cross each other with a barrier of a few $k_B T$. Since the macroscopic properties of the chains are not altered, these two potentials can be used to identify the contribution from the noncrossability of the chains. Note that the general monomer packing constraints are only weakly affected, as the pressure and the temperature for the two models remain the same.

First we studied the mean-square displacements of different monomers, as illustrated in the inset of Fig. 1. This motion can be directly studied by neutron spin-echo experiments [11]. We monitor the motion of the end
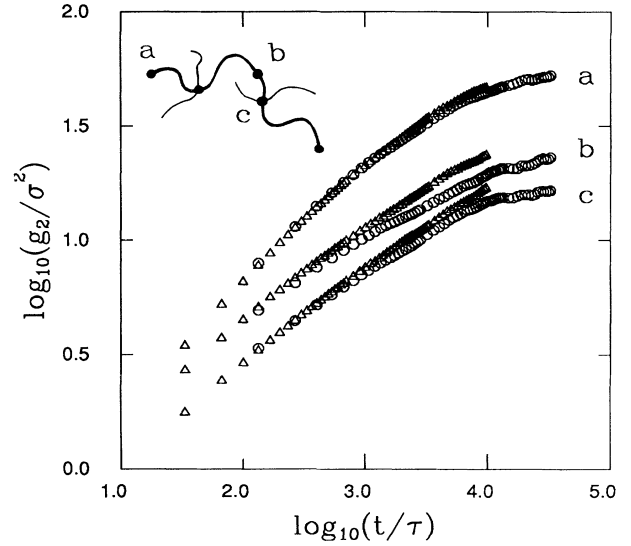
FIG. 1. Mean-square displacement of the chain ends (plot a), middle monomers (b), and cross-links (c) for the two monomer potentials given by Eq. (1) (open circles) and Eq. (3) (triangles) for the 400/50 system.

monomers and the middle monomers (actually the three innermost ones) of the original chains, and the cross-linked monomers which belong to the infinite cluster. Figure 1 shows the mean-square displacements,

$$g_2(t) = \langle \{ [\mathbf{r}_i(t) - \mathbf{R}_{c.m.}(t)] - [\mathbf{r}_i(0) - \mathbf{R}_{c.m.}(0)] \}^2 \rangle. \quad (4)$$

$\mathbf{R}_{c.m.}$ is the center of mass of the percolating network and i denotes an end, middle, or cross-linked monomer. For short times there is no difference between the two potentials, showing that the monomeric friction is identical. For short times the displacement $g_2(t)$ follows the Rouse $t^{1/2}$ law. However, for longer times a significant slowing down occurs for both cases. Comparing these results to our work on melts, it is clear that the crossover to the plateau is extremely slow. Note that the Rouse relaxation time τ_N of a chain in the free melt for subchains of N_s =9 is only 120τ, while for N =50, $\tau_{N=50} \approx 3700\tau$. $g_2(t)$ for the inner monomers of a free chain of length 50 in a melt at $\tau_{N=50}$ is approximately 40σ^2, while for the largest times (t =30000τ) we can follow the system, $g_2(t) \approx 25\sigma^2 \approx 10R_G^2(N_s)$ and extrapolates to a slightly larger value for the middle monomers of the chains interacting via the LJ potential. The slowing down is similar for both potentials. The values of $g_2(t)$ for both potentials start to deviate at $t \approx 100\tau$-400τ, which is slightly larger than the Rouse time of the average strand length. For longer times, the contribution from chain crossing is relevant. A similar but little less pronounced separation occurs for the cross-links where $g_2(t)$ for the cross-links is already greater than $7R_G^2(N_s)$. These results are in clear contrast with the classical picture of rubbers [2]. The dangling ends show a much weaker effect. The ends are too short to display the dominance of

the slow retraction of the dangling strands and the relaxation of the ends cannot explain the extremely slow dynamics as suggested by Curro and Pincus [12]. The distribution of strand lengths and topology dominate the relaxational properties, even though $N_s \approx \frac{1}{4} N_e$. This is also seen very clearly in the single-chain dynamic structure function $S(q,t)$,

$$S(q,t) = \left\langle \sum_{i,j=1,N} \exp\{i\mathbf{q}\cdot[\mathbf{r}_j(t)-\mathbf{r}_i(0)]\} \right\rangle_{|q|}, \quad (5)$$

where i,j run over all monomers of a given chain. The index $|q|$ denotes that the data are averaged over the orientations of $\mathbf{q}$. Figure 2 gives a Rouse plot of $S(q,t)/S(q,0)$ vs $\frac{1}{6}q^2\sqrt{t}$. For Rouse chains the data should fall on a single curve, where the slope directly relates to the monomer friction as found for a melt of free chains (dashed line in Fig. 2). Here we see strong variations from very early times, displaying the slowing down and the effect of the topology. The data decay towards a plateau value, which should correspond to the volume the monomers of the chain can explore. Using this analogy to the reptation model, the tube diameter d_T is between 9σ ($q=0.4$) and 7.7σ ($q=0.8$), roughly the diameter of the chains. However, it is important to note that this effect is very difficult to observe experimentally for the very long times involved. Indeed, a Rouse plot of recent neutron spin-echo data of the motion of the cross-links does not display significant deviations from a single curve [11].

The importance of the topology becomes even more pronounced for the plateau modulus G^0, which is mea-
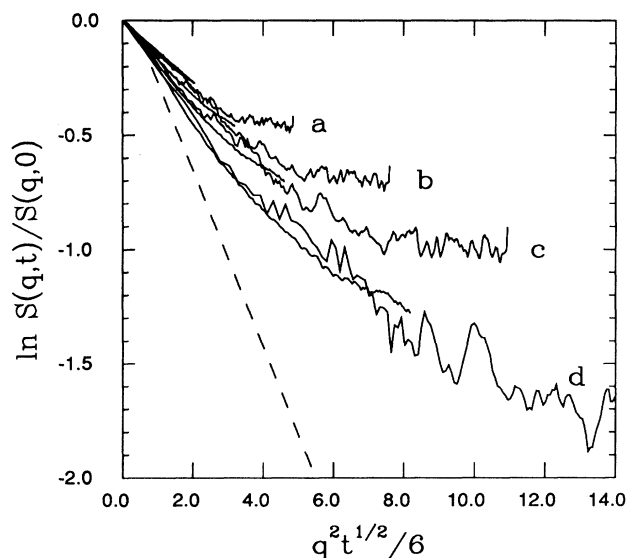
FIG. 2. Dynamic structure function $S(q,t)/S(q,0)$ vs $\frac{1}{6}q^2\sqrt{t}$ for the original chains for the 50/50 and 400/50 systems using the LJ interaction, Eq. (1), for (curve a) $q=0.4$, (b) 0.5, (c) 0.6, and (d) 0.8. The data for the 400/50 system go to long times. The dashed line is the Rouse result for a system of free chains of length $N=50$ [4].

sured by shear experiment, extrapolated to zero shear. G^0 describes the memory of the system and is directly related to the length of elastically active strands in the system. Following Pearson and Graessley [13], G^0 can be written as the sum of two terms,

$$G^0 = [(v-h\mu)/V]k_BT + T_eG_N^0, \quad (6)$$

where V is the total volume of the system. The first term is the entropic contribution. Here v is the number of elastically active strands, μ is the number of elastically active cross-links, and h is an empirical parameter, $0 \le h \le 1$. $h=1$ corresponds to the phantom network model while $h=0$ corresponds to the affine model. Using the standard percolation notation, v and μ correspond to the strands and cross-links of the backbone of the percolating cluster, originating from the assumption that each strand participates equally in sustaining the stress of the system. The second contribution to G^0, $T_eG_N^0$, is the trapping contribution due to the noncrossability of the chains. G_N^0 is the melt plateau modulus for the un-cross-linked system and T_e the trapping factor, which depends only on the gel fraction ϕ_g [13]. Since $G_N^0=0$ for chains of length $N=50$, the trapping factor is expected to be zero. The first contribution was determined by a detailed analysis of the infinite cluster. The average of five smaller 50/50 systems and the large 400/50 system agree within a few percent and give $(v-\mu)k_BT/V=0.013$ ±0.001 for the phantom model and $vk_BT/V=0.034$ ±0.001 for the affine model. In the affine model, G^0 is determined solely from the number of monomers which are elastically active. G^0 can also be written as $G^0 = \rho^*k_BT/N_{\text{eff}}$, where N_{eff} is the effective elastic strand length and ρ^* is the density of monomers supporting stress in the system. Including only those monomers which are elastically active ($\rho^*=0.37$), we find $N_{\text{eff}}=11$.

By using two different potentials we can estimate the contributions of the two terms in Eq. (5) separately under excluded volume conditions. To calculate G^0 we return to the chain structure of the system. Following the standard theories for polymer melts [14], the time-dependent modulus of the system can be calculated from the Rouse eigenmodes of the chains. With $\mathbf{X}_p(t)$ being the pth mode and $A_p(t) = \langle\mathbf{X}_p(t)\mathbf{X}_p(0)\rangle/\langle\mathbf{X}_p^2\rangle$, the autocorrelation function of the pth mode of the modulus is given by

$$G(t) = \frac{\rho k_BT}{N} \sum_{p=1}^{\infty} A_p(2t) \xrightarrow{t\to\infty} \frac{\rho k_BT}{\langle N_s \rangle}. \quad (7)$$

This relation should hold in a melt for chains of many entanglement lengths. Here, however, the original chains consist of only a few strands and a large fraction of monomers are in dangling ends ($\approx 46\%$). The calculation of $G(t)$ directly from the original, short chains leads to an artificially small value for $G^0 = G(t\to\infty)$. To overcome this difficulty we constructed chains which belonged to the infinite cluster with the condition that no part of the constructed chain contained a dangling end.
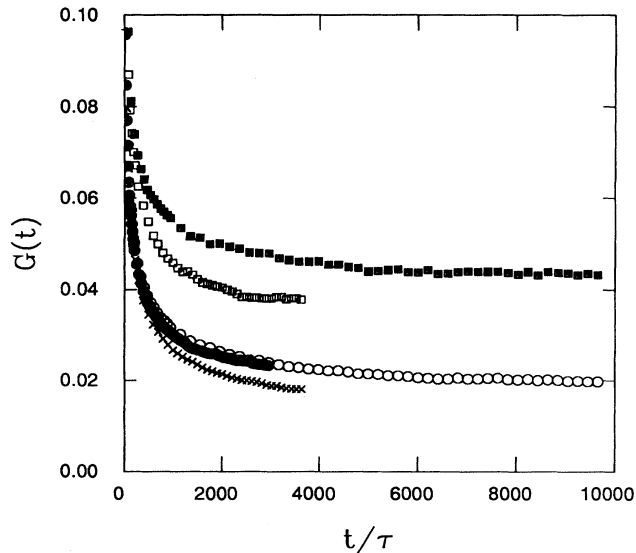
FIG. 3. Time-dependent modulus $G(t)$ for the original chains and the constructed chains for the two potentials. Results for the original chains are given in the lower three curves for the 400/50 system for the LJ (o) and cosine (×) potentials and for the 50/50 system for the LJ potential (●). The upper two curves show the results for the constructed chains for the 400/50 system for the LJ (■) and cosine (□) potentials.

We built chains of lengths 50 and 100. Within our error bars we found no difference in $G(t)$ for the two cases, which are shown in Fig. 3. As expected, the original chains for both potentials give a value of the plateau modulus which is too small. From the constructed chains we find a clear asymptotic plateau modulus for both cases, $G^0_{LJ} = 0.040 \pm 0.002$ for the LJ potential and $G^0_{cos} = 0.031 \pm 0.002$ for the cosine potential. This shows that none of the classical models describe the data very well. Even the affine model, which is expected to give an upper limit, underestimates G^0, while the cosine potential marginally agrees with G^0. Obviously, the excluded volume constraint and the noncrossability of the chains are the reasons for this deviation. This suggests that even though the original chain length N is relatively short, some entanglements are trapped by the cross-links and contribute to G^0.

To summarize, in this paper we have presented the first results in an extensive set of simulations of polymer networks. Using two different interaction potentials, the contributions from the chain trapping can explicitly be extracted. We found that the standard division of G^0 into a phantom or affine network part and a trapping part incorrectly estimates the importance of the chain topology for the cross-linking density employed here. We are presently extending this study to different cross-linking densities as well as to longer chains, where the effect of dangling ends is reduced.

(a)Permanent address.

[1] J. D. Ferry, *Viscoelastic Properties of Polymers* (Wiley, New York, 1980).

[2] P. J. Flory, Proc. R. Soc. London, Ser. A **351**, 351 (1976); S. F. Edwards and T. A. Vilgis, Rep. Prog. Phys. **51**, 243 (1988).

[3] L. R. G. Treolar, *Theory of Rubber Elasticity* (Oxford Univ. Press, Oxford, 1949).

[4] K. Kremer and G. S. Grest, J. Chem. Phys. **92**, 5057 (1990); **94**, 4103(E) (1991).

[5] R. B. Bird, R. C. Armstrong, and O. Hassager, *Dynamics of Polymeric Liquids* (Wiley, New York, 1977), Vol. 1.

[6] M. P. Allen and D. J. Tildesley, *Computer Simulations of Liquids* (Oxford Univ. Press, Oxford, 1987).

[7] E. R. Duering, K. Kremer, and G. S. Grest (to be published).

[8] G. S. Grest and K. Kremer, J. Phys. (Paris) **51**, 2829 (1990).

[9] G. S. Grest and K. Kremer, Macromolecules **23**, 4994 (1990).

[10] A. E. Tonelli and E. Helfand, Macromolecules **7**, 59 (1974); E. Helfand and A. E. Tonelli, Macromolecules **7**, 832 (1974).

[11] R. Oeser, B. Ewen, D. Richter, and B. Farago, Phys. Rev. Lett. **60**, 1041 (1988).

[12] J. G. Curro and P. A. Pincus, Macromolecules **16**, 559 (1983); J. G. Curro, D. S. Pearson, and E. Helfand, Macromolecules **18**, 1157 (1985).

[13] D. S. Pearson and W. W. Graessley, Macromolecules **11**, 528 (1978).

[14] M. Doi and S. F. Edwards, *The Theory of Polymer Dynamics* (Oxford Univ. Press, Oxford, 1986).